Encapsulated therapeutic stem cells implanted in the tumor resection cavity induce cell death in gliomas

Timo M Kauer[1,2], Jose-Luiz Figueiredo[1,2], Shawn Hingtgen[1,2] & Khalid Shah[1–4]

Therapeutically engineered stem cells have shown promise for glioblastoma multiforme (GBM) therapy; however, key preclinical studies are urgently needed for their clinical translation. In this study, we investigated a new approach to GBM treatment using therapeutic stem cells encapsulated in biodegradable, synthetic extracellular matrix (sECM) in mouse models of human GBM resection. Using multimodal imaging, we first showed quantitative surgical debulking of human GBM tumors in mice, which resulted in increased survival. Next, sECM encapsulation of engineered stem cells increased their retention in the tumor resection cavity, permitted tumor-selective migration and release of diagnostic and therapeutic proteins *in vivo*. Simulating the clinical scenario of GBM treatment, the release of tumor-selective S-TRAIL (secretable tumor necrosis factor apoptosis inducing ligand) from sECM-encapsulated stem cells in the resection cavity eradicated residual tumor cells by inducing caspase-mediated apoptosis, delayed tumor regrowth and significantly increased survival of mice. This study demonstrates the efficacy of encapsulated therapeutic stem cells in mouse models of GBM resection and may have implications for developing effective therapies for GBM.

Glioblastoma is the most common primary brain tumor in adults with a very poor prognosis[1–3]. Treatment for GBM is maximal surgical tumor resection (debulking)[4] followed by radiation therapy, with concomitant and adjuvant chemotherapy[5,6]. However, recurrence rates of GBM and the associated patient mortality are nearly 100%. Despite many preclinical studies, most *in vivo* GBM models do not mimic the clinical scenario of surgical debulking and instead focus on treating solid intact intracranial tumors. Therefore, in light of the central role of tumor resection in clinical GBM therapy, development of mouse models of GBM resection are a necessity. In this study we have first developed a mouse resection model of GBM using malignant GBM cells engineered with fluorescent and bioluminescent proteins that allow real time visualization of both growth and resection of tumors *in vivo*, thereby simulating the clinical scenario of GBM resection.

Although resection of the primary tumor mass has shown clinical benefit, adjuvant chemotherapy has provided limited extra benefit[3,6]. One of the main impediments to the efficient delivery of many therapeutic molecules is the blood brain barrier[7] and vascular dysfunction in the tumor[8], which prevent many drugs from reaching brain tumor cells. Additionally, many drugs have short systemic half-lives and peak concentrations, which prevent drugs from ultimately reaching the brain and accumulating to therapeutic concentrations in individual brain tumor cells[9]. One of the approaches to overcome the problem of delivering drugs to intracranial tumors is to develop on-site means of delivering new tumor-specific agents. Stem cells have the ability to home to intracranial pathologies including primary and secondary tumor deposits, making them ideally suited for treatment of both primary and residual GBM cells[10]. Using tumor-specific therapeutic

proteins and advanced imaging agents, we and others have previously demonstrated that engineered human and mouse stem cells home extensively to GBMs and have therapeutic benefits[11–15].

There are several barriers to effectively testing stem cell–based therapeutic interventions in a mouse model of GBM resection, including developing methods to introduce stem cells into the resection cavity to prevent rapid 'washout' of a substantial number of cells by cerebrospinal fluid. Also, it is critical to allow efficient secretion of anti-GBM therapies and retain the ability of stem cells to migrate from the resection cavity into the parenchyma toward invasive tumor deposits. Biodegradable sECMs have been used in various rodent models owing to their ability to provide a physiologic environment that promotes stem cell survival while permitting easy *in vivo* transplantation and cell retention. In models of intracerebral hypoxia-ischemia and traumatic spinal cord injury, sECM acts as the necessary biomechanical substrate for endogenous neuroregeneration by increasing the viability of stem cells and promoting differentiation into neurons[16–18]. Subsequent studies again highlighted the utility of biodegradable scaffolds in facilitating stem cell–based therapy in the CNS[19,20]. Although sECM are ideally suited for introducing therapeutic stem cells into GBM resection cavities, no studies have explored the therapeutic potential of this approach.

In this study we developed and tested sECM-encapsulated diagnostic and therapeutic mouse neural stem cells (NSCs) and human mesenchymal stem cells (MSCs) in culture and *in vivo*. Furthermore, we developed a method of introducing therapeutic stem cells into the resection cavity after GBM surgical debulking and showed the therapeutic efficacy of this approach in malignant and invasive GBM models.

[1]Molecular Neurotherapy and Imaging Laboratory, Massachusetts General Hospital, Harvard Medical School, Boston, Massachusetts, USA. [2]Department of Radiology, Massachusetts General Hospital, Harvard Medical School, Boston, Massachusetts, USA. [3]Department of Neurology, Massachusetts General Hospital, Harvard Medical School, Boston, Massachusetts, USA. [4]Harvard Stem Cell Institute, Harvard University, Cambridge, Massachusetts, USA. Correspondence should be addressed to K.S. (kshah@helix.mgh.harvard.edu).

ARTICLES

RESULTS

Mouse model of GBM resection

To develop a mouse surgical resection model of GBM, we used malignant GBM cells engineered with fluorescent and bioluminescent proteins. Human U87 GBM cells were transduced with lentiviral (LV) construct LV-Fluc-mCherry, sorted and screened for mCherry fluorescent protein (**Fig. 1a**) and firefly luciferase (Fluc) expression (**Fig. 1b**). There was a direct correlation between the Fluc expression and the number of cells (**Fig. 1b**). We then implanted U87-Fluc-mCherry human GBM cells in a cranial window created by removal of a small circular portion of the skull (**Fig. 1c,d**; **Supplementary Fig. 1a,b**) and imaged mice for tumor progression and volume over time by fluorescence intravital microscopy (IVM) and Fluc bioluminescence imaging. We resected established GBM tumors in mice generated by implantation of low (7.5×10^4) and high (1.5×10^5) numbers of GBM cells and used and IVM and BLI imaging to determine the extent of resection (**Fig. 1e–i**). Fluc imaging confirmed more than 60% of the tumor was resected in mice bearing small tumors, whereas more than 80% of the tumor was resected in mice with large tumors that were easier to visualize (**Fig. 1i**; **Supplementary Fig. 1c**). High resolution IVM and hematoxylin and eosin staining further confirmed the efficiency of resection (**Fig. 1e–i**). Kaplan-Meier survival curves showed a significant increase in the survival of mice with resected tumors as compared to the mice with un-resected tumors generated after implanting both low and high numbers of tumor cells (**Fig. 1j**).
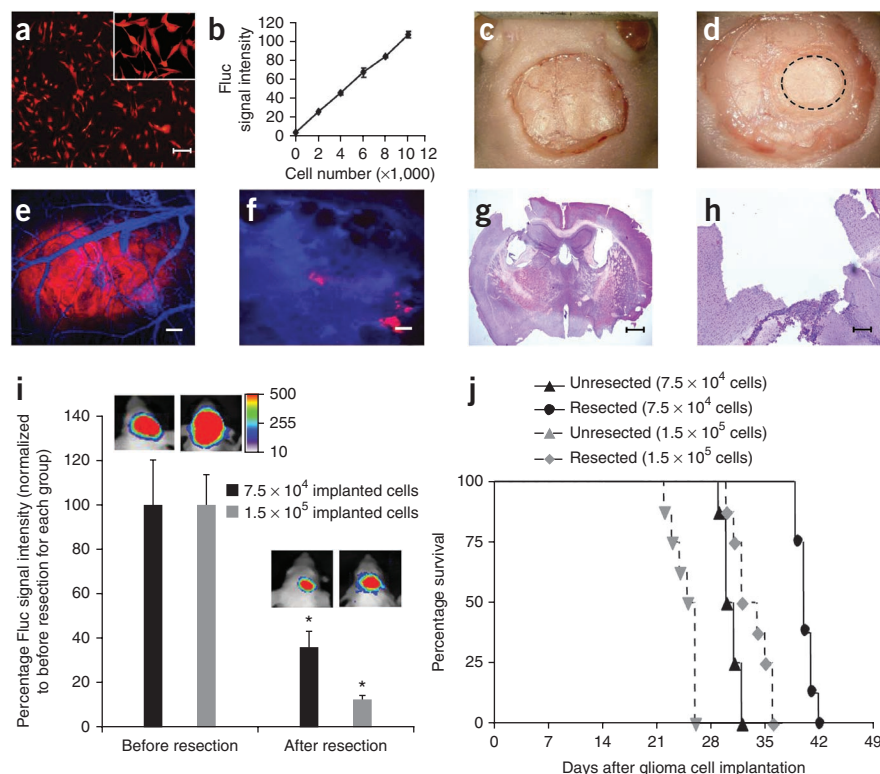
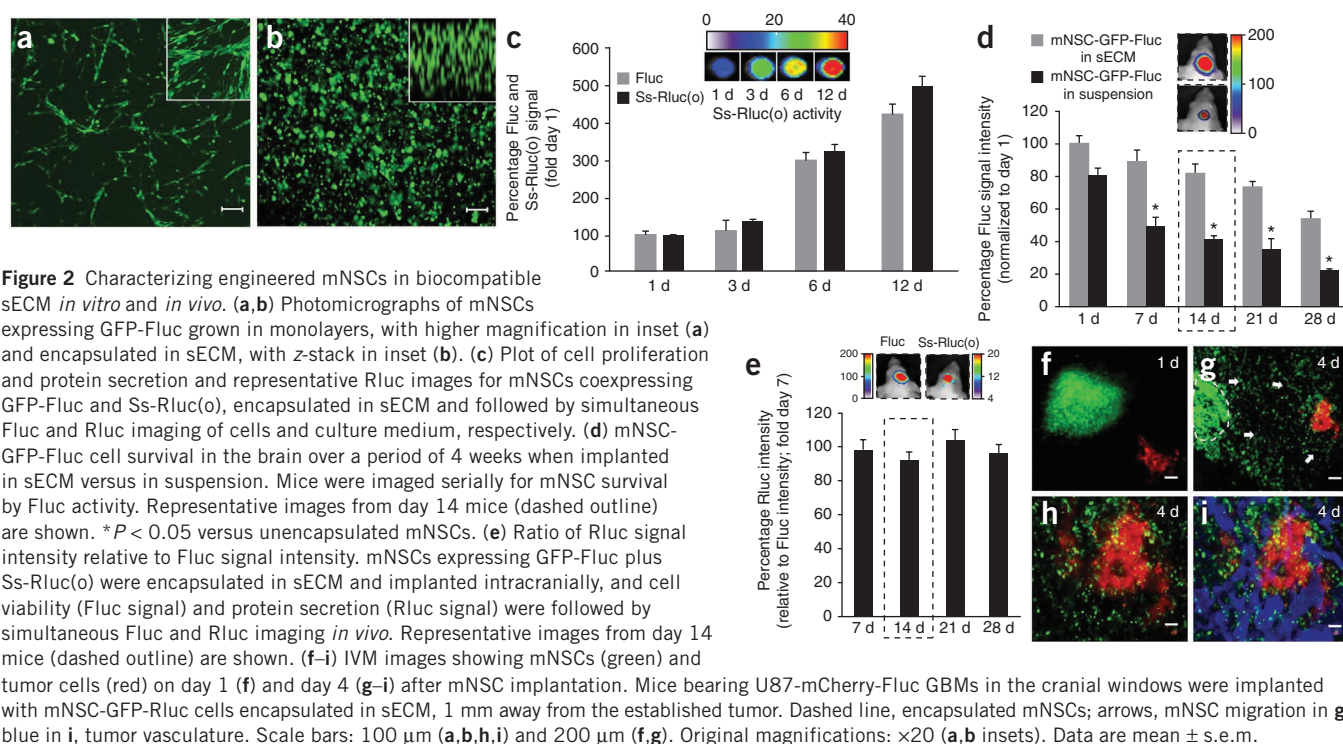### Characterizing mouse NSCs encapsulated in sECM

To assess survival of NSC encapsulated in sECM *in vitro*, we engineered mouse NSCs (mNSCs) to express either GFP-Fluc or to GFP-Fluc plus a secretable *Renilla* luciferase marker, Ss-Rluc(o), using our previously developed diagnostic lentiviral vectors[21,22] (**Fig. 2a**). We confirmed a direct correlation between number of sECM-encapsulated cells and Fluc activity and Ss-Rluc(o) activity *in vitro* (**Supplementary Fig. 2**). Both engineered mNSC types were encapsulated in sECM (**Fig. 2b**), and there was a stable increase in both the cell proliferation (Fluc activity) and protein secretion (Rluc activity) when mNSCs expressing GFP-Fluc plus Ss-Rluc(o) and encapsulated in sECM were cultured over time (**Fig. 2c**). To assess the influence of sECM on cell survival *in vivo*, we implanted mNSC-GFP-Fluc cells in suspension or encapsulated in sECM intracranially and imaged mice serially for mNSC survival by Fluc activity. There was a significantly greater *in vivo* cell viability of sECM-encapsulated mNSCs as compared to the un-encapsulated mNSCs (**Fig. 2d**). To longitudinally monitor mNSC-expressed proteins *in vivo*, we intracranially implanted sECM-encapsulated mNSCs expressing GFP-Fluc plus Ss-Rluc(o) in mice. *In vivo*, dual bioluminescence imaging showed a stable expression of Ss-Rluc(o) from mNSCs over time (**Fig. 2e**). To follow migration of sECM-encapsulated mNSCs, we implanted mice bearing U87-Fluc-mCherry GBMs in a cranial window with mNSC-GFP-Rluc cells encapsulated in sECM 1 mm away from the established tumor. IVM revealed that sECM-encapsulated mNSCs migrated out of the sECM and specifically homed to tumors in the brain over a period of 4 d (**Fig. 2f–i**).

To assess the therapeutic potential of mNSCs expressing therapeutic proteins that specifically kill tumor cells, we engineered mNSCs to express S-TRAIL or its diagnostic variant Di-S-TRAIL or controls. TRAIL is a cytotoxic agent that is known to induce apoptosis in about 50% of GBM[23,24]. We showed a similar response of established and primary GBM lines to S-TRAIL–mediated apoptosis *in vitro*

Figure 1 Tumor resection prolongs survival of mice bearing GBM. (**a,b**) Cell transduction. Human U87 GBM cells were transduced with LV-Fluc-mCherry, and cells were imaged 48 h later for mCherry expression and Fluc activity. Photomicrograph of U87 cells expressing Fluc-mCherry (**a**) and plot revealing the correlation between U87-Fluc-mCherry cell number and Fluc activity (**b**). (**c–f**) Cranial implantation. A cranial window was established in mice and U87-Fluc-mCherry cells (7.5×10^4 or 1.5×10^5) were implanted in the cranial window. Light images of the mouse skull with skin removed (**c**), drilled rim around the cranial window (**d**). Dashed circle indicates the tumor growing area in the cranial window. (**e,f**) IVM. Mice with established U87-Fluc-mCherry GBMs in the cranial window were injected with a blood-pool agent, AngioSense-750. Photomicrographs before (**e**) and after (**f**) tumor resection (red, tumor; blue, vasculature). (**g,h**) Photomicrographs of low (**g**) and high (**h**) magnification hematoxylin and eosin staining of brain sections showing tumor resection cavity. (**i**) Plot of the Fluc signal intensity and representative visible light plus superimposed bioluminescence images (color scale units, photons min^{-1} cm^{-2}; here and in subsequent figures) before and after tumor resection in mice implanted with 7.5×10^4 (resected 14 d after implantation) or 1.5×10^5 (resected 21 d after implantation) GBM cells. *$P < 0.05$ versus before resection for each group. Data are mean ± s.e.m. (**j**) Kaplan-Meier survival curves of mice with and without resected U87-Fluc-mCherry tumors. $P < 0.05$ resected versus un-resected tumors for each group. Scale bars, 100 µm (**a,e,f,h**) and 400 µm (**g**). Original magnifications: ×2 (**c**) and ×4 (**d**).

Figure 2 Characterizing engineered mNSCs in biocompatible sECM *in vitro* and *in vivo*. (**a**,**b**) Photomicrographs of mNSCs expressing GFP-Fluc grown in monolayers, with higher magnification in inset (**a**) and encapsulated in sECM, with *z*-stack in inset (**b**). (**c**) Plot of cell proliferation and protein secretion and representative Rluc images for mNSCs coexpressing GFP-Fluc and Ss-Rluc(o), encapsulated in sECM and followed by simultaneous Fluc and Rluc imaging of cells and culture medium, respectively. (**d**) mNSC-GFP-Fluc cell survival in the brain over a period of 4 weeks when implanted in sECM versus in suspension. Mice were imaged serially for mNSC survival by Fluc activity. Representative images from day 14 mice (dashed outline) are shown. *$P < 0.05$ versus unencapsulated mNSCs. (**e**) Ratio of Rluc signal intensity relative to Fluc signal intensity. mNSCs expressing GFP-Fluc plus Ss-Rluc(o) were encapsulated in sECM and implanted intracranially, and cell viability (Fluc signal) and protein secretion (Rluc signal) were followed by simultaneous Fluc and Rluc imaging *in vivo*. Representative images from day 14 mice (dashed outline) are shown. (**f**–**i**) IVM images showing mNSCs (green) and tumor cells (red) on day 1 (**f**) and day 4 (**g**–**i**) after mNSC implantation. Mice bearing U87-mCherry-Fluc GBMs in the cranial windows were implanted with mNSC-GFP-Rluc cells encapsulated in sECM, 1 mm away from the established tumor. Dashed line, encapsulated mNSCs; arrows, mNSC migration in **g**; blue in **i**, tumor vasculature. Scale bars: 100 μm (**a**,**b**,**h**,**i**) and 200 μm (**f**,**g**). Original magnifications: ×20 (**a**,**b** insets). Data are mean ± s.e.m.

(**Supplementary Fig. 3**). There was a significant reduction in GBM cell viability when mNSC-S-TRAIL cells encapsulated in sECM were placed in the culture dish containing the TRAIL-sensitive human GBM cells U87-Fluc-mCherry (**Fig. 3a**–**e**). The decrease in GBM cell viability was associated with an increase in caspase-3/7 activity (**Fig. 3e**) and changes in caspase-8 and polyADP-ribose polymerase (PARP) activity (**Fig. 3f**; **Supplementary Fig. 4**). S-TRAIL ELISA confirmed a high TRAIL concentration (150–650 ng ml^{-1}) in the culture medium containing mNSC-S-TRAIL cells encapsulated in sECM (**Supplementary Fig. 5**). To simultaneously monitor release of S-TRAIL from sECM-encapsulated mNSCs and its effect on GBM cell viability in sECM-encapsulated mNSCs cultured with U87-mCherry-Fluc GBM cells, we engineered mNSCs with Di-S-TRAIL. Dual bioluminescence imaging showed robust levels of Di-S-TRAIL released from sECM that increased as the stem cell/tumor cell ratio increased and resulted in a significant and dose-dependent decrease in GBM cell viability (**Fig. 3g**). These results show that sECM-encapsulated engineered mNSCs survive longer in mice brains, migrate to tumors in the brain and induce apoptosis in cultured GBM cells.

Therapeutic effect of 'armed' stem cells *in vivo*

To assess survival of mNSCs encapsulated in sECM in mouse model of GBM resection, we implanted mNSC-GFP-Fluc cells, either in suspension or encapsulated, in the resection cavity of U87 GBMs. sECM-encapsulated mNSCs were retained in the tumor resection cavity (**Fig. 4a**–**c**) at high local concentrations adjacent to the residual tumor cells (**Fig. 4d**). sECM-encapsulated mNSC survival in the tumor resection cavity over a period of 1 month was significantly higher than that of the unencapsulated mNSCs in the resection cavity (**Fig. 4e**). Next, to assess the therapeutic potential of sECM-encapsulated mNSC-S-TRAIL cells in mouse resection models of GBM, we implanted sECM-encapsulated mNSC-S-TRAIL or mNSC-GFP-Rluc cells intracranially in the tumor resection cavity and followed mice for changes in tumor volume by serial Fluc bioluminescence imaging

and for survival. sECM-encapsulated mNSC-S-TRAIL cells induced a marked increase in caspase-3/7 activity and a >80% decrease in residual tumor cells as early as 3 d after seeding that could be followed by simultaneously visualizing caspase-3/7 activation and tumor volumes serially *in vivo* (**Fig. 4f**). Notably, sECM-encapsulated mNSC-S-TRAIL cells suppressed regrowth of residual tumor cells through 49 d after resection (**Supplementary Fig. 6**). Highlighting the survival benefit of this approach, mice treated with control sECM-encapsulated mNSC-GFP-Rluc cells showed a median survival of 14.5 d after GBM resection. In contrast, 100% of mice treated with mNSC-S-TRAIL cells encapsulated in sECM after GBM resection were alive 42 d after treatment (**Fig. 4g**). sECM encapsulation was required for the survival benefit, as mNSC-S-TRAIL cells delivered in suspension into the resection cavity conferred no significant increase in survival (**Fig. 4g**). These results reveal that sECM-encapsulated therapeutic mNSCs are retained in the tumor resection cavity, kill residual GBM cells and thus result in significantly increased survival of mice.

Several studies have shown that freshly isolated primary glioma lines from clinical specimens more accurately recapitulate the clinical scenario of GBMs. To assess the clinical relevance of sECM-encapsulated stem cell–based therapeutic regimen in a more clinically relevant model, we used a TRAIL-sensitive primary human invasive glioma line, GBM8, and human bone marrow–derived MSCs (hMSCs). We engineered GBM8 cells to express a mCherry-Fluc fusion protein and showed that the GBM8-mCherry-Fluc line retained the tumor cell invasive properties of the parental line in culture (**Fig. 5a**) and *in vivo* (**Fig. 5b**). There was a direct correlation between the Fluc signal intensity and the number of cells *in vitro* in the ranges tested (**Supplementary Fig. 7**). To assess the migration and the therapeutic potential of hMSCs expressing therapeutic proteins that specifically kill tumor cells, we engineered hMSCs to express GFP or S-TRAIL and GFP. In cultures of sECM-encapsulated hMSCs with GBM8 cells, hMSCs expressing GFP only or S-TRAIL migrated out of the sECM and tracked GBM8 cells (**Fig. 5c**–**f**). Furthermore, hMSC-S-TRAIL
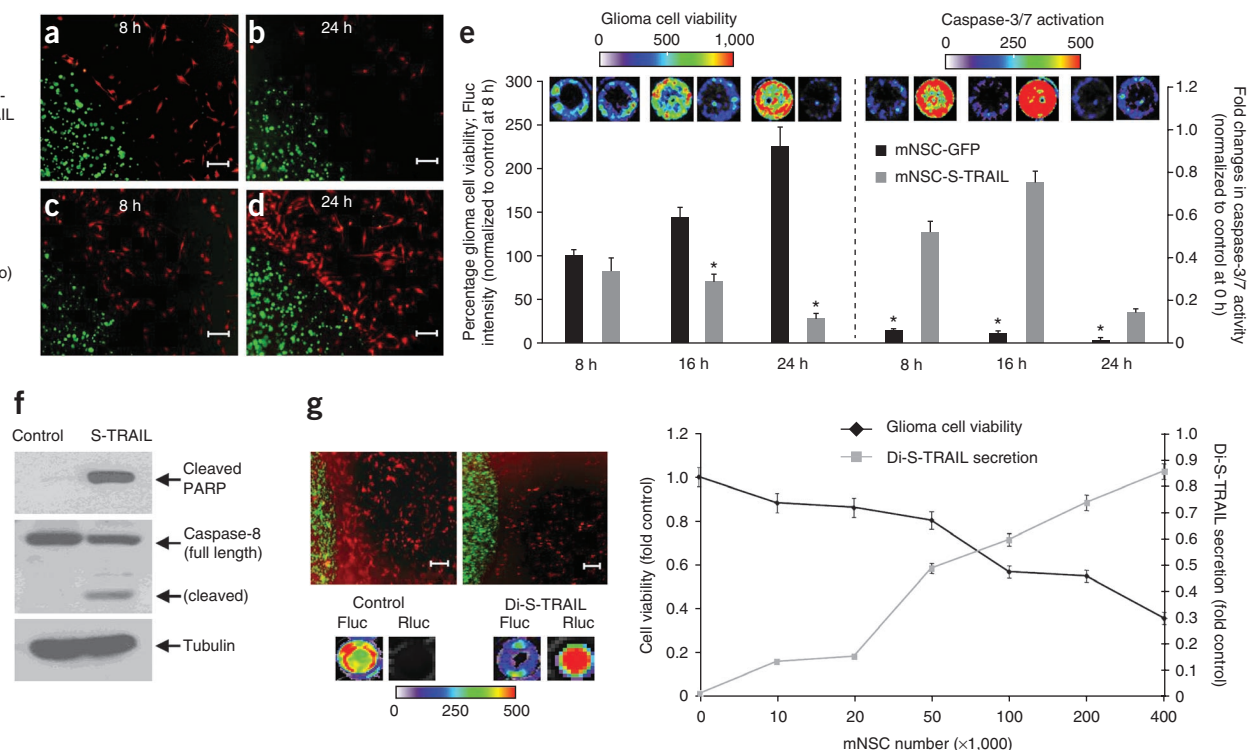
Figure 3 mNSCs expressing therapeutic S-TRAIL induce GBM cell death *in vitro*. (**a**–**e**) mNSCs (green) expressing Ss-Rluc(o) or S-TRAIL were encapsulated in sECM and placed in a culture dish containing human GBM U87-Fluc-mCherry cells (red). Photomicrographs show sECM-encapsulated mNSCs at 8 h (**a**,**c**) and 24 h (**b**,**d**). Plot shows tumor cell viability (*$P < 0.05$ versus controls) and caspase-3/7 activation (*$P < 0.05$ versus mNSC-S-TRAIL) over 24 h when cultured with either sECM-encapsulated mNSC-GFP or mNSC-S-TRAIL cells (**e**). (**f**) Western blot analysis on GBM cells collected 8 h after sECM-encapsulated mNSC-S-TRAIL or mNSC-GFP (control) cell placement in the culture dish (see **Supplementary Fig. 4** for uncropped blots). (**g**) Representative images and summary graph demonstrating the effect of the release of Di-S-TRAIL from sECM-encapsulated mNSCs cultured with U87-mCherry-Fluc cells at increasing ratios of stem cell to tumor cell. After 24 h of culture, fluorescence photomicrographs (top left) were taken, Di-S-TRAIL was visualized by Rluc bioluminescence imaging and tumor cell viability was visualized by Fluc bioluminescence imaging. Scale bars, 100 μm. Data are mean ± s.e.m.

cells induced GBM8 cell death in a time- (**Fig. 5g**) and caspase-3/7–dependent (2.7 ± 0.1 fold increase in caspase-3/7 activity in comparison to hMSC-GFP cells) manner. Next, to assess the therapeutic potential of sECM-encapsulated hMSC-S-TRAIL cells in mouse resection models of primary GBM8 tumors, we implanted sECM-encapsulated hMSC-S-TRAIL or hMSC-GFP cells intracranially in a GBM8 tumor resection cavity and followed mice for changes in tumor volume by serial Fluc bioluminescence imaging. The presence of sECM-encapsulated hMSC-S-TRAIL cells resulted in significantly less residual GBM8 cells than in the controls (**Fig. 5h**). Fluorescence imaging of brain sections revealed the presence of encapsulated hMSCs in the tumor resection cavity and also suggested hMSCs migration to invading glioma cells (**Fig. 5i,j**). Histopathological analysis on brain sections revealed a significantly higher number of cleaved caspase-3–positive cells in hMSC-S-TRAIL–treated mice than in controls (**Fig. 5k,l**; 4.2 ± 0.2 fold increase in the hMSC-S-TRAIL group versus the hMSC-GFP group). These results show that sECM-encapsulated engineered human MSCs have therapeutic benefits against primary tumor-derived GBMs.

DISCUSSION

In this study we tested diagnostic and therapeutic stem cells encapsulated in sECM in a mouse model of GBM resection. We show that sECM encapsulation of stem cells significantly increased their retention time in the GBM resection cavity, permitted robust tumor-selective migration and allowed secretion of anti-tumor proteins from

sECM-encapsulated stem cells *in vivo*. Furthermore, we show that TRAIL-secreting sECM-encapsulated stem cells transplanted in the resection cavity significantly delayed tumor regrowth in mice bearing established (U87) and primary invasive (GBM8) GBMs and significantly increased survival of mice bearing established GBMs.

The clinical standard of care for patients suffering from GBMs includes surgical debulking[3,6], yet nearly all preclinical models focus on treating established solid tumors. Previously, a few studies have shown the feasibility of resecting established GBMs in different animal models[25,26]. In this study, we expanded the results of previous studies by integrating fluorescent and bioluminescent markers and extensive optical imaging to simultaneously confirm the presence of established tumors, visualize the extent of tumor resection and serially monitor tumor regrowth after resection. The inclusion of post-resection bioluminescence imaging permitted gross assessment of total tumor removal, and real-time fluorescence microscopy permitted visualization of residual tumor cells and associated blood vessels in resected tumors. The combination of quantitative, noninvasive imaging and GBM resection should allow continued optimization of the resection model and further the exploration of anti-GBM therapeutics using mouse models with greater clinical relevance than current xenograft models that are focused on treating solid tumor masses.

Despite extensive preclinical evidence demonstrating the potential of cell-based therapy for GBM, no preclinical studies have explored methods to introduce therapeutically 'armed' stem cells in GBM resection cavities. The exploration of such methods is

Figure 4 sECM-encapsulated mNSC-S-TRAIL cells transplanted into the tumor resection cavity increase survival of mice. (**a**) Light photomicrograph of the resection cavity containing sECM-encapsulated mNSCs (outlined area). (**b–d**) mNSC-GFP-Fluc cells encapsulated in sECM were implanted intracranially in the resection cavity, and the mice were injected with Angiosense-750 (blue) intravenously and imaged by IVM and by serial Fluc bioluminescence imaging. (**b**) Fluorescence photomicrograph showing mNSCs (green) targeting residual GBM cells (red) in a tumor resection cavity with leaky vasculature (blue). (**c**) Hematoxylin and eosin image of sECM-encapsulated mNSC-GFP-Fluc cells implanted (outlined area) in the resection cavity. (**d**) Higher magnification fluorescence photomicrograph showing mNSCs (green) targeting residual GBM cells (red) indicated by arrows in a tumor resection cavity with leaky vasculature (blue). (**e**) Plot and representative images from day 7 (dashed outlines) of the relative mean Fluc signal intensity of mNSC-GFP-Fluc cells in suspension or encapsulated in sECM, placed in the GBM resection cavity (*$P < 0.05$ versus encapsulated mNSCs). (**f,g**) mNSC-S-TRAIL or mNSC-GFP-Rluc cells encapsulated in sECM or mNSC-S-TRAIL cells in suspension were implanted intracranially in the tumor resection cavity. (**f**) TRAIL-mediated caspase-3/7 activation and tumor volumes as assessed by serial bioluminescence imaging after aminoluciferin and luciferin injections, respectively. Caspase-3/7 activity, *$P < 0.05$ versus mNSC-S-TRAIL; tumor volumes, *$P < 0.05$ versus controls. (**g**) Kaplan-Meier survival curves. $P < 0.05$, resected + GFP-Rluc cells in sECM versus un-resected; $P < 0.05$, resected + mNSC-S-TRAIL cells in sECM versus resected + mNSC-S-TRAIL cells in suspension. Scale bars, 200 μm (**b**) and 100 μm (**c,d**). Original magnification, ×4 (**a**). Data are mean ± s.e.m.
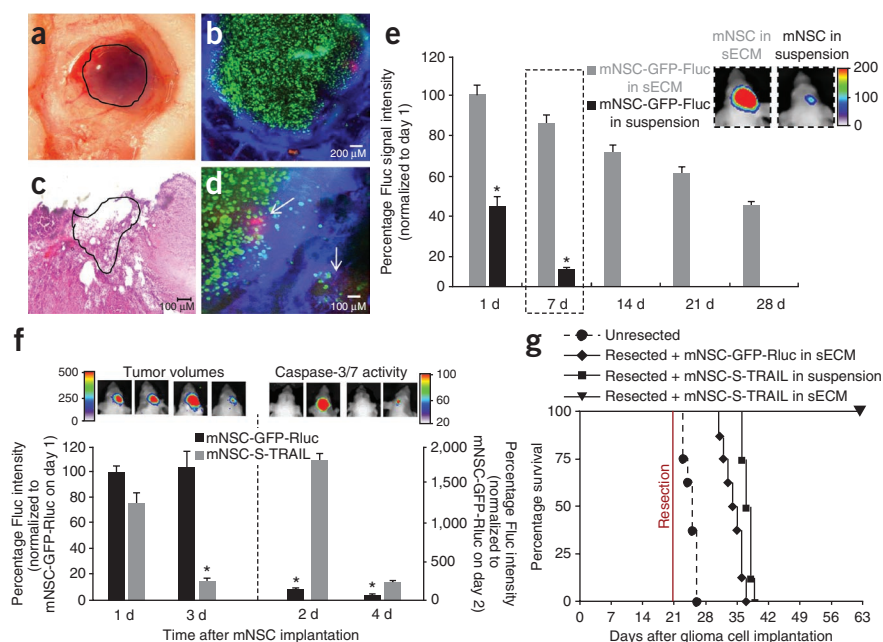
vital to prevent stem cell 'washout' and rapid diffusion from the resection cavity by cerebrospinal fluid while allowing release of anti-tumor proteins directly into the resection cavity from the transplanted stem cells. Biodegradable sECM formulations are an attractive approach for retention of stem cells in the resection cavity. Several previous studies have shown that biodegradable sECM increase the viability of mNSCs and their differentiation into neurons *in vitro*[16]. Recent *in vivo* studies suggest considerable potential for transplanted biodegradable scaffolds containing stem (and other neuronal) cells in models of degeneration and hypoxia-ischemia[27]. In this study we have used sECMs that are based on a thiol-modified hyaluronic acid and a thiol reactive cross-linker (polyethylene glycol diacrylate), which provides biocompatibility, physiological relevance and customizability[28]. Additionally, release profiles of sECM used in this study were well suited to permit both migratory stem cells and secreted therapeutic proteins to exit the sECM. These events were confirmed by serial monitoring of diagnostic markers (luciferase and fluorescence), which revealed that mNSCs migrated extensively out of the sECM toward GBM while secreting high levels of diagnostic proteins. We also observed that sECM encapsulation markedly increased the survival of mNSCs in resection cavities as compared to non-sECM-encapsulated cells over a period of 4 weeks. Although the precise reason for the increased survival of sECM-encapsulated mNSCs is unclear, studies have demonstrated that sECM encapsulation can enhance survival of transplanted cells by providing a physiologically relevant environment that promotes attachment to reduce anoikis-mediated death, reduce cell diffusion, and provide protection from the host immune system[29,30]. Our study clearly reveals that sECM-encapsulated engineered mNSCs are effective at extending the drug exposure time of tumor cells, by means of retaining high concentrations of therapeutic stem cells at the site of tumor resection.

In our previous studies, we have shown that human NSCs have significantly shorter survival after implantation than mouse NSCs

in nude mice bearing intracranial tumors[22]. As long-term survival of stem cells in mouse brains was critical for fully evaluating the therapeutic effects of encapsulated therapeutic NSCs, therefore we used primary mouse NSCs as opposed to human NSCs for most of our studies.

The ability of TRAIL to selectively target tumor cells while remaining harmless to most normal cells[10,23,24,31] makes it an attractive candidate for an apoptotic therapy for highly malignant GBMs. Sustained levels of TRAIL are key to improving the efficiency and potency of TRAIL-based proapoptotic cancer therapy, and several studies have previously demonstrated that TRAIL-expressing human and mouse stem cells have therapeutic benefits[11–15,32]. In our recent studies, we have shown that mNSCs do not express TRAIL receptors and are insensitive to TRAIL-mediated apoptosis[33]. Using a diagnostic variant of S-TRAIL, our results clearly reveal that mNSC-secreted S-TRAIL is released from sECM and induces caspase-3–mediated apoptosis in GBM cells *in vitro*. When encapsulated into sECM and implanted into resected GBM tumors, mNSC-S-TRAIL cells resulted in a significant increase in survival of mice bearing GBMs. These results confirm that TRAIL is a potent inhibitor of brain tumor growth and that encapsulated mNSC-S-TRAIL cytotoxic therapy is highly efficient in inducing apoptosis in residual GBM cells in our mouse model of GBM resection. Furthermore, stem cells have the advantage of offering a continuous and concentrated local delivery of secretable therapeutic molecules like TRAIL, thus reducing the nonselective targeting and allowing higher treatment efficiency and potency for a longer time period.

Although TRAIL is a selective and potent anti-tumor agent, many tumor lines, including some established GBM lines, have varying resistance or sensitivity to TRAIL-induced apoptosis, with about 50% of already established GBM lines being resistant to TRAIL[23,24] (also see **Supplementary Fig. 3**). Although therapy with sECM-encapsulated TRAIL-secreting stem cells will be efficacious for TRAIL-sensitive
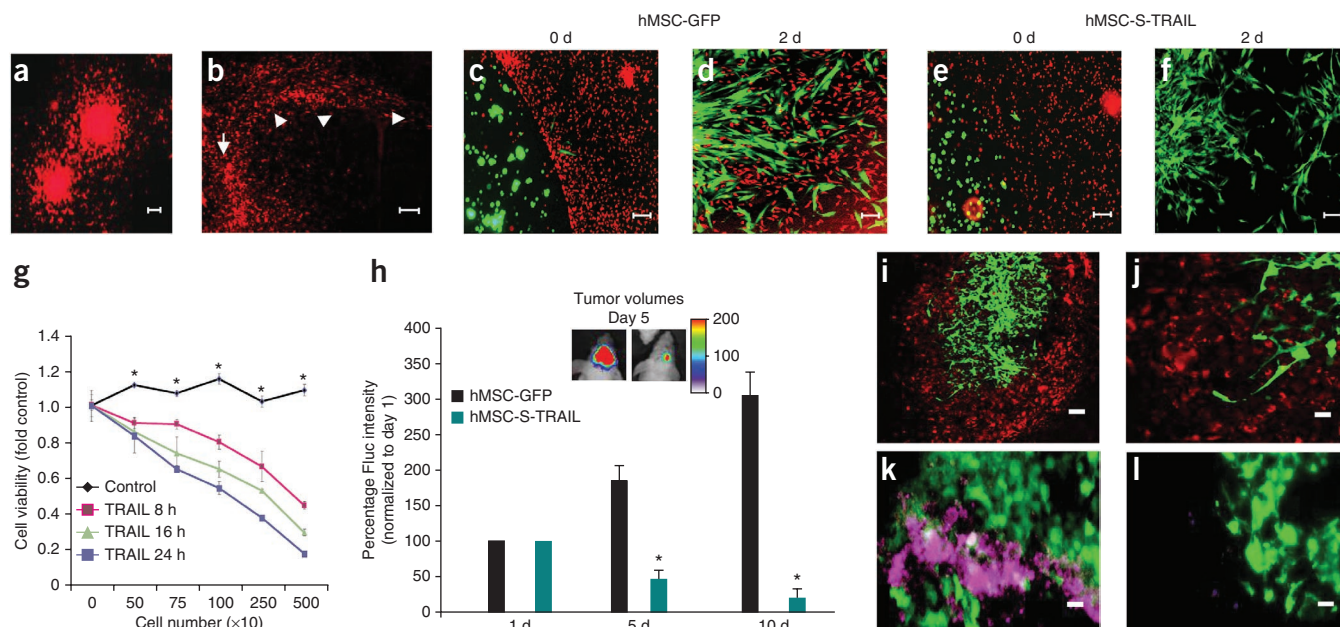
Figure 5 sECM-encapsulated therapeutic human MSCs have anti-tumor effects on primary invasive human GBMs *in vitro* and *in vivo*. (**a,b**) Primary invasive GBM8-mCherry-Fluc cells grown as neurospheres in a collagen matrix (**a**) and brain section of mice bearing GBM8-mCherry-Fluc tumors, showing the highly invasive nature of GBM8 (**b**). Arrow, site of implantation; arrowheads, path of invasion. (**c–g**) hMSCs expressing GFP or S-TRAIL were encapsulated in sECM and placed in a culture dish containing human GBM8-Fluc-mCherry cells. hMSCs (green) were followed for migration out of sECM, and GBM8 cells (red) were followed for their response to S-TRAIL secreted by hMSCs. Photomicrographs show sECM-encapsulated hMSCs on the day of plating (**c,e**) and 48 h after plating (**d,f**). (**g**) GBM8 cell viability at different time points after culturing with varying numbers of either sECM-encapsulated hMSC-GFP (control) or hMSC-S-TRAIL (TRAIL) cells. *$P < 0.05$ versus TRAIL at 8 h, 16 h and 24 h. (**h–j**) Encapsulated hMSC-S-TRAIL or hMSC-GFP cells in sECM were implanted intracranially in the tumor resection cavity of mice bearing GBM8-mCherry-Fluc cells and mice were followed for changes in tumor volume by serial Fluc bioluminescence imaging and correlative immunohistochemistry. Plot and representative images show the relative mean Fluc signal intensity from mice bearing sECM-encapsulated hMSC-GFP or hMSC-S-TRAIL cells. *$P < 0.05$ versus control (**h**). (**i,j**) Low-magnification (**i**) and high-magnification (**j**) photomicrographs of serial brain sections of mice showing hMSCs (green) on day 5 after hMSC implantation in the GBM8 (red) resection cavity. (**k,l**) Representative images showing cleaved caspase-3 staining (purple) on brain sections from mice implanted with hMSC-S-TRAIL cells (green, **k**) and control cells (green, **l**) 5 d after treatment. Scale bars: 100 μm (**a,c–f,i**), 200 μm (**b**) and 50 μm (**j–l**). Data are mean ± s.e.m.

GBMs, many GBM tumors are likely to be fully resistant to TRAIL-based therapies. To address GBMs that are fully resistant to TRAIL, many *in vitro* studies have shown the potential of sensitizing TRAIL-resistant GBM cell lines to TRAIL-mediated apoptosis by treatment with agents including temozolomide[21], protease inhibitors[34], cisplatin[35], proteasome inhibitors[36] and daidzein[37]. Recent *in vivo* studies have shown that treatment with irradiation followed by TRAIL-secreting umbilical cord blood–derived MSCs synergistically enhances apoptosis in TRAIL-sensitive and TRAIL-resistant GBM[38]. Although these studies hold promise, it would be ideal to use stem cells that simultaneously secrete different therapeutic proteins that target multiple pathways in GBMs as the only source of therapy. Along these lines, we have engineered stem cells to secrete an anti-angiogenic agent consisting of three type-1 anti-angiogenic repeats of thrombospondin-1 (aaTSP-1) and shown in a recently published study that prolonged release of aaTSP-1 from stem cells in mice bearing gliomas targets GBM-associated vasculature and increases mouse survival[39]. As TSP-1 is known to normalize vasculature and upregulate death receptors DR4 and DR5 on tumor associated endothelial cells[40], the use of stem cells expressing TRAIL and TSP-1 offers the potential to augment TRAIL-mediated apoptosis in both GBM cells and associated endothelial cells. We anticipate that the continued development of new stem cell–delivered, targeted anti-tumor agents and the use of systemically delivered sensitizing agents with stem cell–delivered TRAIL might ultimately allow treatment of both TRAIL-resistant and TRAIL-sensitive GBM tumor types.

The limited availability of noninvasive methods to monitor multiple molecular events has been one of the main limitations in testing the efficacy of various tumor therapy protocols. In our previous studies, we have shown that we can follow delivery of NSCs[22] and MSCs[32] and quantify GBM burden *in vivo*[22,41] using noninvasive bioluminescence imaging. Combining bioluminescence imaging and confocal IVM offers great potential to image events serially. In this study, we have labeled tumor cells and stem cells with bimodal imaging markers (bioluminescent and fluorescent) expressed as a single transcript, which expands the number of events that can be visualized *in vivo*, and efficiently applied bioluminescence imaging to follow both un-resected and resected intracranial tumors and the fate of NSCs *in vivo*. To follow pharmacokinetics of therapeutic S-TRAIL both in culture and in mouse models of GBM, we have also used a C-terminal fusion of S-TRAIL with Ss-Rluc(o), which we recently engineered and characterized for its extracellular functionality[33]. In addition, we have also used a blood-pool agent, AngioSense-750, to visualize the tumor-associated vasculature. The inclusion of noninvasive molecular imaging allows characterization of multiple events in sECM-stem cell therapy with enhanced spatial and temporal resolution. Although the optical imaging methods used in this study are ideally suited for preclinical studies, further studies validating this approach incorporating clinical imaging modalities such as MRI will ease the translation of our approach to the clinic.

In recent years, primary GBM lines have been created from isolated human brain tumor tissue and used for preclinical studies.

Several studies have shown that xenografts of these primary cell lines often recapitulate clinical GBM more faithfully than established GBM cell lines, thus providing more insights and a more stringent test of promising new anti-GBM therapies[42,43]. In developing this study, we initially used an established glioma line, U87, that our laboratory and others have extensively characterized for *in vivo* tumor formation and assessment of target therapeutics in mouse models of brain tumors[21,32,41–44]. Most of the established glioma lines, including U87, form solid intracranial tumors in most cases. This was essential for resection of the primary mass and for study of the effect of sECM-encapsulated mouse stem cells on the residual tumor cells after resection. However, to test the efficacy of sECM-encapsulated stem cell therapy in mouse models of GBM that recapitulate all the features of the human cancer, we used the primary cell line GBM8. We and others have shown GBM8 cells form highly invasive tumors upon intracerebral implantation into mice[32], thus recapitulating most of the features of human GBM. Although primary invasive lines are potentially more predictive, they introduce the technical difficulty of resecting invasive tumor cells from the brain. To circumvent this, we implanted ten times as many GBM8-mCherry-Fluc cells as used by us in previous reports[43] to create an initial solid tumor mass which could then be resected. In addition to a more clinically relevant tumor model, we also used bone marrow–derived hMSCs that have been extensively used in past and ongoing clinical trials (reviewed in ref. 15) and offer the potential of autologous transplantation, thus overcoming the limitation of immune rejection. Pairing the clinically relevant GBM and hMSC lines allowed us to perform extensive studies investigating the effect of encapsulated therapeutic hMSCs in invasive mouse model of GBM resection. Our results clearly showed that hMSC-S-TRAIL cells rapidly attenuated progression of GBM8 tumors in the brains of mice. Because of the clinical relevance of the models used in our study, our approach could be effective for treating patients suffering from GBM. However before translating these therapies to GBM patients, it is critical to use the most appropriate stem cell source and also to assess the long-term fate of these cells[15,45].

Although most studies, including our previous studies in mouse models of GBM, have shown that human bone marrow–derived MSCs offer the potential of autologous transplantation and have antitumor therapeutic potential (reviewed in ref. 15), some studies have suggested tumor-promoting properties in mouse tumor models[46,47] and mass formation in an experimental autoimmune encephalomyelitis model in mice[48]. As the tumorigenic potential of different stem cell types remains a potential concern, the use of alternative stem cell sources, including adipose tissue–derived MSCs[49] and skin-derived reprogrammed induced pluripotent NSCs (reviewed in ref. 50) from patients, should be considered. Alternatively, the incorporation of suicide genes such as HSV-TK into therapeutic human stem cell types would ultimately allow the eradication of therapeutic stem cells after GBM treatment. These approaches should eliminate any potential for malignant neoplasm formation from stem cells and heighten their safety for clinical applications.

In conclusion, our studies reveal the fate and therapeutic efficacy of engineered and sECM-encapsulated mouse and human stem cells in a mouse model of GBM resection. Using this study as a template, advances can be made in the way stem cells can be engineered and used clinically in patients with GBM. We envisage that, after the neurosurgical removal of the main tumor mass, the patient's own reprogrammed cells or MSCs, therapeutically engineered with antitumor agent(s) that eradicate GBMs, will be encapsulated in sECM and implanted in the resection cavity of the tumor. These cells would result in the death of both residual and invasive tumor cells, with the ultimate goal of improving patient outcomes. This study could also facilitate translation of stem cell–based therapies for the treatment of many other brain pathologies.

METHODS

Methods and any associated references are available in the online version of the paper at http://www.nature.com/natureneuroscience/.

Note: Supplementary information is available on the Nature Neuroscience website.

AUTHOR CONTRIBUTIONS
K.S. and T.M.K. designed research; T.M.K., J.-L.F., S.H. and K.S. performed research; T.M.K., S.H. and K.S. analyzed data and wrote the paper.

1. Adamson, C. *et al.* Glioblastoma multiforme: a review of where we have been and where we are going. *Expert Opin. Investig. Drugs* **18**, 1061–1083 (2009).
2. Affronti, M.L. *et al.* Overall survival of newly diagnosed glioblastoma patients receiving carmustine wafers followed by radiation and concurrent temozolomide plus rotational multiagent chemotherapy. *Cancer* **115**, 3501–3511 (2009).
3. Wen, P.Y. & Kesari, S. Malignant gliomas in adults. *N. Engl. J. Med.* **359**, 492–507 (2008).
4. Asthagiri, A.R., Pouratian, N., Sherman, J., Ahmed, G. & Shaffrey, M.E. Advances in brain tumor surgery. *Neurol. Clin.* **25**, 975–1003, viii–ix (2007).
5. Erpolat, O.P. *et al.* Outcome of newly diagnosed glioblastoma patients treated by radiotherapy plus concomitant and adjuvant temozolomide: a long-term analysis. *Tumori* **95**, 191–197 (2009).
6. Minniti, G. *et al.* Radiotherapy plus concomitant and adjuvant temozolomide for glioblastoma in elderly patients. *J. Neurooncol.* **88**, 97–103 (2008).
7. Muldoon, L.L. *et al.* Chemotherapy delivery issues in central nervous system malignancy: a reality check. *J. Clin. Oncol.* **25**, 2295–2305 (2007).
8. Jain, R.K., Tong, R.T. & Munn, L.L. Effect of vascular normalization by antiangiogenic therapy on interstitial hypertension, peritumor edema, and lymphatic metastasis: insights from a mathematical model. *Cancer Res.* **67**, 2729–2735 (2007).
9. Sarin, H. Recent progress towards development of effective systemic chemotherapy for the treatment of malignant brain tumors. *J. Transl. Med.* **7**, 77 (2009).
10. Corsten, M.F. & Shah, K. Therapeutic stem-cells for cancer treatment: hopes and hurdles in tactical warfare. *Lancet Oncol.* **9**, 376–384 (2008).
11. Balyasnikova, I.V., Ferguson, S.D., Han, Y., Liu, F. & Lesniak, M.S. Therapeutic effect of neural stem cells expressing TRAIL and bortezomib in mice with glioma xenografts. *Cancer Lett.* **310**, 148–159 (2011).
12. Ehtesham, M. *et al.* Induction of glioblastoma apoptosis using neural stem cell-mediated delivery of tumor necrosis factor-related apoptosis-inducing ligand. *Cancer Res.* **62**, 7170–7174 (2002).
13. Germano, I.M., Uzzaman, M., Benveniste, R.J., Zaurova, M. & Keller, G. Apoptosis in human glioblastoma cells produced using embryonic stem cell-derived astrocytes expressing tumor necrosis factor-related apoptosis-inducing ligand. *J. Neurosurg.* **105**, 88–95 (2006).
14. Menon, L.G. *et al.* Human bone marrow-derived mesenchymal stromal cells expressing S-TRAIL as a cellular delivery vehicle for human glioma therapy. *Stem Cells* **27**, 2320–2330 (2009).
15. Shah, K. Mesenchymal stem cells engineered for cancer therapy. *Adv. Drug Deliv. Rev.* doi:10.1016/j.addr.2011.06.010 (29 June 2011).
16. Pan, L., Ren, Y., Cui, F. & Xu, Q. Viability and differentiation of neural precursors on hyaluronic acid hydrogel scaffold. *J. Neurosci. Res.* **87**, 3207–3220 (2009).
17. Park, K.I., Teng, Y.D. & Snyder, E.Y. The injured brain interacts reciprocally with neural stem cells supported by scaffolds to reconstitute lost tissue. *Nat. Biotechnol.* **20**, 1111–1117 (2002).
18. Teng, Y.D. *et al.* Functional recovery following traumatic spinal cord injury mediated by a unique polymer scaffold seeded with neural stem cells. *Proc. Natl. Acad. Sci. USA* **99**, 3024–3029 (2002).
19. Ma, W. *et al.* CNS stem and progenitor cell differentiation into functional neuronal circuits in three-dimensional collagen gels. *Exp. Neurol.* **190**, 276–288 (2004).
20. Potter, W., Kalil, R.E. & Kao, W.J. Biomimetic material systems for neural progenitor cell-based therapy. *Front. Biosci.* **13**, 806–821 (2008).

21. Hingtgen, S. *et al.* Targeting multiple pathways in gliomas with stem cell and viral delivered S-TRAIL and Temozolomide. *Mol. Cancer Ther.* **7**, 3575–3585 (2008).

22. Shah, K. *et al.* Bimodal viral vectors and *in vivo* imaging reveal the fate of human neural stem cells in experimental glioma model. *J. Neurosci.* **28**, 4406–4413 (2008).

23. Panner, A., James, C.D., Berger, M.S. & Pieper, R.O. mTOR controls FLIPS translation and TRAIL sensitivity in glioblastoma multiforme cells. *Mol. Cell. Biol.* **25**, 8809–8823 (2005).

24. Rieger, J., Naumann, U., Glaser, T., Ashkenazi, A. & Weller, M. APO2 ligand: a novel lethal weapon against malignant glioma? *FEBS Lett.* **427**, 124–128 (1998).

25. Akbar, U. *et al.* Delivery of temozolomide to the tumor bed via biodegradable gel matrices in a novel model of intracranial glioma with resection. *J. Neurooncol.* **94**, 203–212 (2009).

26. de Oliveira, M.S. *et al.* Anti-proliferative effect of the gastrin-release peptide receptor antagonist RC-3095 plus temozolomide in experimental glioblastoma models. *J. Neurooncol.* **93**, 191–201 (2009).

27. Orive, G., Anitua, E., Pedraz, J.L. & Emerich, D.F. Biomaterials for promoting brain protection, repair and regeneration. *Nat. Rev. Neurosci.* **10**, 682–692 (2009).

28. Xu, X., Yang, G., Zhang, H. & Prestwich, G.D. Evaluating dual activity LPA receptor pan-antagonist/autotaxin inhibitors as anti-cancer agents *in vivo* using engineered human tumors. *Prostaglandins Other Lipid Mediat.* **89**, 140–146 (2009).

29. Mooney, D.J. & Vandenburgh, H. Cell delivery mechanisms for tissue repair. *Cell Stem Cell* **2**, 205–213 (2008).

30. Terrovitis, J. *et al.* Ectopic expression of the sodium-iodide symporter enables imaging of transplanted cardiac stem cells *in vivo* by single-photon emission computed tomography or positron emission tomography. *J. Am. Coll. Cardiol.* **52**, 1652–1660 (2008).

31. Ashkenazi, A. & Dixit, V.M. Death receptors: signaling and modulation. *Science* **281**, 1305–1308 (1998).

32. Sasportas, L.S. *et al.* Assessment of therapeutic efficacy and fate of engineered human stem cells for cancer therapy. *Proc. Natl. Acad. Sci. USA* **106**, 4822–4827 (2009).

33. Hingtgen, S.D., Kasmieh, R., van de Water, J., Weissleder, R. & Shah, K. A novel molecule integrating therapeutic and diagnostic activities reveals multiple aspects of stem cell-based therapy. *Stem Cells* **28**, 832–841 (2010).

34. Tian, X. *et al.* Modulation of chop-dependent DR5 expression by nelfinavir sensitizes glioblastoma multiforme cells to tumor necrosis factor-related apoptosis-inducing ligand (TRAIL). *J. Biol. Chem.* **286**, 29408–29416 (2011).

35. Chen, J., Sun, X., Yang, W., Jiang, G. & Li, X. Cisplatin-enhanced sensitivity of glioblastoma multiforme U251 cells to adenovirus-delivered TRAIL *in vitro*. *Tumour Biol.* **31**, 613–622 (2010).

36. Kahana, S. *et al.* Proteasome inhibitors sensitize glioma cells and glioma stem cells to TRAIL-induced apoptosis by PKCε-dependent downregulation of AKT and XIAP expressions. *Cell. Signal.* **23**, 1348–1357 (2011).

37. Siegelin, M.D., Gaiser, T., Habel, A. & Siegelin, Y. Daidzein overcomes TRAIL-resistance in malignant glioma cells by modulating the expression of the intrinsic apoptotic inhibitor, bcl-2. *Neurosci. Lett.* **454**, 223–228 (2009).

38. Kim, S.M. *et al.* Irradiation enhances the tumor tropism and therapeutic potential of tumor necrosis factor-related apoptosis-inducing ligand-secreting human umbilical cord blood-derived mesenchymal stem cells in glioma therapy. *Stem Cells* **28**, 2217–2228 (2010).

39. van Eekelen, M. *et al.* Human stem cells expressing novel TSP-1 variant have anti-angiogenic effect on brain tumors. *Oncogene* **29**, 3185–3195 (2010).

40. Ren, B. *et al.* A double hit to kill tumor and endothelial cells by TRAIL and antiangiogenic 3TSR. *Cancer Res.* **69**, 3856–3865 (2009).

41. Kock, N., Kasmieh, R., Weissleder, R. & Shah, K. Tumor therapy mediated by lentiviral expression of shBcl-2 and S-TRAIL. *Neoplasia* **9**, 435–442 (2007).

42. Pandita, A., Aldape, K.D., Zadeh, G., Guha, A. & James, C.D. Contrasting *in vivo* and in vitro fates of glioblastoma cell subpopulations with amplified EGFR. *Genes Chromosom. Cancer* **39**, 29–36 (2004).

43. Wakimoto, H. *et al.* Human glioblastoma-derived cancer stem cells: establishment of invasive glioma models and treatment with oncolytic herpes simplex virus vectors. *Cancer Res.* **69**, 3472–3481 (2009).

44. Bagci-Onder, T., Wakimoto, H., Anderegg, M., Cameron, C. & Shah, K. A dual PI3K/mTOR inhibitor, PI-103, cooperates with stem cell-delivered TRAIL in experimental glioma models. *Cancer Res.* **71**, 154–163 (2011).

45. Snyder, E.Y. The risk of putting something where it does not belong: Mesenchymal stem cells produce masses in the brain. *Exp. Neurol.* **230**, 75–77 (2011).

46. Hall, B. *et al.* Mesenchymal stem cells in cancer: tumor-associated fibroblasts and cell-based delivery vehicles. *Int. J. Hematol.* **86**, 8–16 (2007).

47. Karnoub, A.E. *et al.* Mesenchymal stem cells within tumour stroma promote breast cancer metastasis. *Nature* **449**, 557–563 (2007).

48. Grigoriadis, N. *et al.* Variable behavior and complications of autologous bone marrow mesenchymal stem cells transplanted in experimental autoimmune encephalomyelitis. *Exp. Neurol.* **230**, 78–89 (2011).

49. Choi, S.A. *et al.* Human adipose tissue-derived mesenchymal stem cells: characteristics and therapeutic potential as cellular vehicles for prodrug gene therapy against brainstem gliomas. *Eur. J. Cancer* published online, doi:10.1016/j.ejca.2011.04.033 (8 June 2011).

50. Mattis, V.B. & Svendsen, C.N. Induced pluripotent stem cells: a new revolution for clinical neurology? *Lancet Neurol.* **10**, 383–394 (2011).

ONLINE METHODS

Cell lines. Human glioma lines U87, LN229, A172, U251, Gli36vIII, Gli79, LN319 and U87 and primary GBM8-EF, GBM4, GBM6, GBM18 and BT74 cells were grown as described previously[32,41,43,44]. Primary mouse neural stem cells (kindly provided by A. Vescovi, University of Milan) were grown in NSC Basal medium (Stem Cell Technologies) supplemented with proliferation supplements (Stem Cell Technologies) and epidermal growth factor (20 ng ml^{-1}, R&D Systems) as previously described[33]. Adherent cultures were established by culturing mNSCs on tissue culture plates coated with laminin and poly-ornithine (Sigma). Human bone marrow–derived MSCs (kindly provided by D. Prockop, Tulane University) were grown as described previously[32].

Engineered cell lines and tumor cell viability assays. The following lentiviral vectors were used in this study: LV-GFP, LV-GFP-Fluc, LV-GFP-Rluc, LV-Rluc-DsRed2 (ref. 22), Pico-mCherry-Fluc (kindly provided by A. Kung, Dana-Farber Cancer Center), LV-Ss-Rluc(o)[33], LV-S-TRAIL[41] and LV-Di-S-STRAIL[33]. Both LV-S-TRAIL and LV-Di-S-TRAIL have an IRES (internal ribosomal entry site)-GFP element in the coding sequence. All lentiviral constructs were packaged as lentiviral vectors in 293T/17 cells using a helper virus–free packaging system as described previously[41]. Stem cells and GBM cells were transduced with lentiviruses at varying multiplicity of infection by incubating virions in a culture medium containing 4 µg ml^{-1} protamine sulfate (Sigma) and cells were visualized for fluorescent protein expression by fluorescence microscopy. After expansion in culture, both stem cells and GBM cells were sorted by fluorescence-activated cell sorting (FACSAria Cell Sorting System, BD Biosciences). The effects of different concentrations of S-TRAIL on established and primary GBM cell viability were measured using an ATP-dependent luminescence reagent (CellTiterGlo, Promega).

sECM-encapsulated NSCs: cell viability, ELISA and release of secreted proteins. The sECM components, Hystem and Extralink (Glycosan Hystem-C, Biotime Inc.), were reconstituted according to the manufacturer's protocol. mNSCs (1×10^5, 2×10^5 or 4×10^5) expressing either GFP-Fluc and Ss-Rluc(o) or S-TRAIL were resuspended in Hystem (14 µl) and the matrix was cross-linked by adding Extralink (6 µl). After 20 min (gelation time) at 25 °C, the mNSC-sECM hydrogel was placed in the center of different sizes (35 or 60 mm) of glass-bottomed dish.

To determine the correlation between the number of U87-Fluc-mCherry or sECM-encapsulated mNSCs expressing GFP-Fluc or Ss-Rluc(o) and the bioluminescence signal, different numbers of mNSCs were encapsulated in sECM and U87-mCherry-Fluc cells were seeded in different concentrations and imaged as described previously[33]. Each experiment was performed in triplicate. To simultaneously assess mNSC viability and release of mNSC-secreted proteins from the sECM, mNSCs expressing GFP-Fluc and Ss-Rluc(o) were encapsulated in sECM and followed by Fluc and Rluc bioluminescence imaging *in vitro* as described previously[33] over a period of 12 d. To assess TRAIL concentration, the conditioned medium from sECM-encapsulated mNSCs expressing Ss-Rluc(o) or S-TRAIL was collected and ELISA was performed as described previously[41].

***In vitro* imaging of S-TRAIL secretion, tumor cell viability and caspase-3/7 activity.** mNSCs expressing Ss-Rluc(o) or S-TRAIL (1×10^5) were encapsulated in sECM and placed in a 35-mm plate as described above. Human U87-mCherry-Fluc GBM cells (2×10^5) were plated around the sECM-encapsulated mNSCs, and GBM cell viability at different time points (8–24 h) was measured by quantitative *in vitro* bioluminescence imaging as described previously[33]. GBM cells were also assessed at different time points (8–24 h) for caspase-3/7 activity with a caged, caspase-3/7–activatable DEVD-aminoluciferin (Caspase-Glo 3/7, Promega) as described previously[32]. For coculture experiments, increasing numbers ($0-4 \times 10^5$) of mNSCs expressing Di-S-TRAIL were encapsulated in sECM and plated, and U87-mCherry-Fluc cells (1×10^5) were seeded around the sECM-encapsulated mNSCs 24 h later. After coculture for 24 h, the medium was transferred to a new plate, combined with coelenterazine (1 µg ml^{-1}) and imaged to quantify Di-S-TRAIL. At the same time, 1.5 µg ml^{-1} D-luciferin was added to the remaining GBM cells and GBM cell viability was determined by Fluc bioluminescence imaging. Similarly, hMSCs expressing GFP or S-TRAIL (1×10^5) were encapsulated in sECM and placed in a 35-mm plate, GBM8-mCherry-Fluc cells (2×10^5) were plated around the sECM-encapsulated hMSCs, and cell viability and caspase-3/7 activity were measured by quantitative *in vitro* bioluminescence imaging at different time points (15–24 h) as described above.

Western blot analysis. Human U87 GBM cells were incubated with conditioned medium from sECM-encapsulated mNSCs expressing S-TRAIL or Ss-Rluc(o) for 18 h, lysed and centrifuged at 30,000*g* for 30 min at 4 °C. Equal amounts of total cellular protein (30 µg) were denatured, separated by SDS-PAGE, transferred to nitrocellulose membrane, blocked and incubated for 1 h at 25 °C with rabbit polyclonal antibodies to cleaved PARP and caspase-8 (Cell Science). Blots were developed using enhanced chemiluminescence reagents (Amersham). Membranes were then exposed to film for 30 s to 30 min.

Collagen invasion assay. Human GBM8-Fluc-mCherry cells created from the GBM8-EF line were grown as spheres and resuspended in rat tail collagen, type 1 (BD Biosciences). The solution was then allowed to solidify in a culture dish and the cells were supplemented with the growth medium as described earlier[32]. Collagen-embedded GBM8-Fluc-mCherry cells were imaged at days 0 and 5 to visualize the dispersal of GBM8-Fluc-mCherry cells into the collagen matrix from the primary sphere.

Creation of a mouse model of resection. Athymic nude mice (6–8 weeks of age; Charles River Laboratories) 25–30 g in weight ($n = 8$ in each group) were used for the intracranial xenograft GBM model. One week before GBM cell implantation, mice were immobilized on a stereotactic frame, a small circular portion of the skull (~7 mm diameter) was removed and the dura was gently peeled back from the cortical surface. U87-expressing Fluc-mCherry were collected at 80% confluency and implanted stereotactically (7.5×10^4 or 1.5×10^5; $n = 16$ in each case) in the right frontal lobe, and the skin was sutured. On the day of tumor resection (day 14 after tumor cell implantation for mice implanted with 7.5×10^4 tumor cells, day 21 for mice implanted with 1.5×10^5 cells; $n = 16$ in each group), mice were imaged by Fluc bioluminescence imaging ($n = 16$ from each group) and IVM ($n = 3$ in each group) as described previously[22]. For IVM, Angiosense-750 (Visen Medical) was injected and mice were imaged to visualize tumor volumes and associated vasculature as described previously[39]. For tumor resection, mice ($n = 8$ from each group) were immobilized on a stereotactic frame, the skin was opened and the superficial tumor was exposed. A dissecting Leica surgical microscope with ×20 magnification was used for mechanical resection to reduce the tumor volume up to the tumor-tissue interface, leaving margins of the dura intact. Finally, the wound was copiously irrigated and the skin closed with 4-0 Vicryl suture. Mice were imaged by bioluminescence imaging and IVM after resection. *Ex vivo* analysis on resected tumors was performed by incubating tumors in PBS containing 1.5 µg ml^{-1} D-luciferin and by bioluminescence imaging. All *in vivo* procedures were approved by the Subcommittee on Research Animal Care at Massachusetts General Hospital. This study used 140 female mice.

sECM-encapsulated mNSC survival, migration and therapeutic efficacy studies. To compare sECM-encapsulated and unencapsulated mNSC survival in athymic nude mice, GFP-Fluc–expressing mNSCs (5×10^5 per mouse) were either resuspended in PBS or encapsulated in sECM and implanted stereotaxically ($n = 5$ in each case) in the right frontal lobe (from bregma, −2 mm anterior–posterior; from midline, 2 mm lateral; from dura, 2 mm ventral) and mice were imaged on weeks 1–4 for Fluc activity as described below. To compare sECM-encapsulated and unencapsulated mNSC survival in the tumor resection cavity, mice implanted with U87-Rluc-DsRed2 tumors in the cranial window were imaged for Rluc activity by injecting 100 µg of coelenterazine per mouse through the tail vein (described in detail below), tumors were resected and mice were implanted with GFP-Fluc–expressing mNSCs (5×10^5 per mouse) either resuspended in PBS or encapsulated in sECM ($n = 5$ in each case). To encapsulate mNSCs expressing GFP-Fluc, mNSCs were resuspended with sECM components described above and, 10 min later, the encapsulated mNSC-sECM mix was placed in the resection cavity immediately after tumor resection and the skin was closed with 4-0 Vicryl suture. Mice were imaged on weeks 1–4 for Fluc activity as described below and IVM as described above. To study the migration of sECM-encapsulated mNSCs toward GBMs, U87-mCherry-Fluc cells (5×10^4) were implanted stereotaxically into the right frontal lobe in cranial windows of nude mice ($n = 10$) and, 7 d later, encapsulated mNSC-GFP-Fluc cells ($n = 5$) or saline ($n = 5$) were injected 1 mm lateral to the tumor implantation site. mNSCs migration was followed by IVM as described earlier[22].

To study the effect of therapeutic mNSC-S-TRAIL cells encapsulated in sECM in the resection model, mice ($n = 32$) bearing U87-mCherry-Fluc GBMs in the

cranial window were imaged for Fluc activity on the day of resection (day 21 after tumor cell implantation) and divided into four groups (n = 8 in each group) by distributing mice of matching tumor sizes (indicated by the Fluc signal intensity) equally across all groups, and tumors were resected (n = 24) as described above. Mice were imaged for Fluc signal intensity immediately after resection. sECM-encapsulated mNSC-S-TRAIL (n = 8) or mNSC-GFP-Rluc cells (n = 8) or unencapsulated mNSC-S-TRAIL cells (n = 8) were placed in the tumor resection cavity and mice were followed for survival over time, as were un-resected controls (n = 8). Tumor volumes in the mNSC-S-TRAIL and mNSC-GFP-Rluc groups were imaged by Fluc bioluminescence imaging as described earlier[32]. To study the effect of therapeutic hMSC-S-TRAIL cells encapsulated in sECM in the primary invasive GBM8 resection model, mice (n = 14) bearing GBM8-mCherry-Fluc tumors in the cranial window were imaged for Fluc activity on the day of resection (day 7 after tumor cell implantation) and divided into two groups (n = 7 in each group) as described above. sECM-encapsulated hMSC-S-TRAIL (n = 7) or hMSC-GFP (n = 7) cells were placed in the tumor resection cavity and tumor volumes were imaged by Fluc bioluminescence imaging as described earlier[32].

Dual bioluminescence imaging *in vivo*. To simultaneously visualize survival of encapsulated mNSCs and release of Ss-Rluc(o), mNSCs expressing GFP-Fluc and Ss-Rluc(o) were implanted in the frontal lobe of nude mice (n = 6) as described above. For dual luciferase imaging 7, 14, 21 and 28 d after implantation, mice were injected with 100 μg of coelenterazine per mouse through the tail vein and imaged for Ss-Rluc(o) activity as described previously[32]. Eighteen hours later, when there was no residual coelenterazine-Rluc activity, mice were injected with 1 mg D-luciferin per mouse intraperitoneally and imaged for Fluc activity

5 min later as described above. Postprocessing and visualization were performed as described previously[32]. To simultaneously visualize tumor volumes and caspase-3/7 activity, mice bearing U87-mCherry-Fluc tumors were resected and implanted with encapsulated mNSC-TRAIL or mNSC-GFP-Rluc cells in the resection cavity. Tumor volumes were followed by imaging mice for Fluc activity as described above. For imaging apoptosis induced by S-TRAIL expression, mice were injected intraperitoneally with highly purified Caspase-Glo 3/7 reagent (5 mg in 150 μl DMSO) and imaged for caspase-3–dependent luciferase activity for 5 min after administration of the Caspase-Glo 3/7 reagent. Postprocessing and visualization were performed as described previously[33]. All images are the visible light image superimposed with bioluminescence images with a scale in photons min^{-1} cm^{-2}.

Tissue processing. Mice bearing tumors in the cranial window or mice with resected tumors or mice with resected tumors and implanted with sECM-encapsulated mNSCs or hMSCs were perfused with formalin and brains were removed and sectioned. Cleaved caspase-3 immunohistochemical staining on brain sections was performed as described earlier[32]. Photomicrographs of immunohistochemistry and hematoxylin and eosin slides were taken using a Nikon E400 light microscope attached to a SPOT CCD digital camera (Diagnostics Instruments).

Statistical analysis. Data were analyzed by Student t-test when comparing two groups and by ANOVA, followed by Dunnett's post-test, when comparing more than two groups. Data are expressed as mean ± s.e.m., and differences were considered significant at $P < 0.05$. Survival times of groups of mice were compared using a log-rank test.